OPEN

Original article

Nuclear Medicine Communications

Glucose-corrected standardized uptake value in the differentiation of high-grade glioma versus post-treatment changes

Asae Nozawa[a,d,e], Ali Hosseini Rivandi[a], Masayuki Kanematsu[e], Hiroaki Hoshi[e], David Piccioni[b,c], Santosh Kesari[b,c] and Carl K. Hoh[a]

Background **Standardized uptake values (SUVs) of fluorine-18 fluorodeoxyglucose PET (^{18}F-FDG PET) are used widely to differentiate residual or recurrent high-grade gliomas from post-treatment changes in patients with brain tumors. The aim of this study is to assess the accuracy of SUV corrected by blood glucose level (SUV_{gluc}) compared with various quantitative methods in this role.**

Materials and methods **In 55 patients with dynamic ^{18}F-FDG PET scans, there were 97 glioma lesions: glioblastoma ($n = 60$), grade III gliomas ($n = 22$), grade III or IV gliomas ($n = 6$), grade I/II ($n = 7$), and prebiopsy lesions ($n = 2$). The final actual diagnosis was made on the basis of pathology ($n = 33$) and clinical outcome ($n = 64$). Dynamic ^{18}F-FDG PET scans were processed to generate parametric images of SUV_{gluc}, SUV_{max}, and glucose metabolic rate (GMR). Lesion to cerebellum ratios (SUV_{Rc}) and contralateral white matter ratios (SUV_{Rw}) were also measured. The SUV_{gluc} was calculated as $SUV_{max} \times$ blood glucose level/100.**

Results **Using the thresholds of $SUV_{max} > 4.6$, $SUV_{Rc} > 0.9$, $SUV_{Rw} > 1.8$, $SUV_{gluc} > 4.3$, and GMR > 12.2 μmol/min/100 g to represent positivity for viable tumors, the accuracies were the same for the SUV_{gluc} and SUV_{Rw} (80%) and were higher than the conventional SUV_{max} (72%). The area under the receiver operating characteristic curve for the SUV_{gluc} (0.8933) was better than that for the SUV_{max} (0.8266) ($P < 0.01$) and was similar to those of the GMR (0.8622), SUV_{Rc} (0.8606), and SUV_{Rw} (0.8981).**

Conclusion **These results suggest that SUV_{gluc} may aid in the differentiation of residual or recurrent high-grade tumor from post-treatment changes in patients with abnormal blood glucose levels. The simplicity of the SUV_{gluc} avoids the complexity of kinetic analysis or the requirement of a reference tissue.** ***Nucl Med Commun*** **36:573–581**

Nuclear Medicine Communications 2015, **36**:573–581

Keywords: fluorine-18 fluorodeoxyglucose, glucose-corrected standardized uptake value, high-grade glioma, PET

Departments of [a]Radiology, [b]Neurosciences, UC San Diego, [c]Translational Neuro-Oncology Laboratories, Moores Cancer Center, UC San Diego Health System, La Jolla, California, USA, [d]Department of Diagnostic Radiology, Gifu Prefectural General Medical Center and [e]Department of Radiology, Gifu University, Gifu, Japan

Correspondence to Carl K. Hoh, MD, UCSD Medical Center, 200 W. Arbor Drive, San Diego, CA 92103-8758, USA
Tel: +1 619 543 6641; fax: +1 619 543 1975; e-mail: ckhoh@ucsd.edu

Received 8 December 2014 **Revised** 15 January 2015
Accepted 15 January 2015

Introduction

High-grade glioma is the most common primary brain tumor in adults. Until recently, treatment options for patients with high-grade glioma were limited and mainly included surgery and radiation therapy. Previously, chemotherapy played a marginal role and was used as an adjuvant treatment or when there was recurrence [1]. Recently, concurrent and adjuvant temozolomide therapy in combination with radiation therapy after surgery has been shown to improve the survival rates of patients with high-grade glioma [2]. However, even after various multidisciplinary approaches, tumors frequently recur, presenting as new enhanced lesions and/or signal abnormalities in the T2-weighted images and diffusion-weighted images in conventional MRI [2,3]. The detection of high-grade gliomas by serial MRI may be the current clinical standard of practice; however, differentiation between high-grade gliomas and post-treatment changes, such as radiation necrosis, or other treatment effects may be difficult as post-treatment-related changes may mimic high-grade tumors. This imaging pattern on MRI can result in challenging interpretations that impact clinical management decisions. To overcome this difficulty, fluorine-18 fluorodeoxyglucose (^{18}F-FDG) PET imaging has been considered to be a modality that helps provide reliable pathophysiologic and diagnostic data in this clinical setting [4].

The accuracy of ^{18}F-FDG PET using dynamic image acquisition and tracer kinetic modeling has been reported previously [5,6]. The model divides ^{18}F-FDG uptake into three compartments with flux rates characterized by kinetic parameters (k_1, k_2, k_3, and k_4). As ^{18}F-FDG is a

DOI: 10.1097/MNM.0000000000000288

Table 1 Enrollment summary

Participant summary	Number of scans
Scans approached	230
Ineligible because nonglioma cases	88
Scans enrolled	142
Ineligible because of disqualification	42
Ineligible because of hyperglycemia and metformin on board	3
Scans with complete data	97

glucose analog, similar kinetic characteristics for endogenous glucose can be calculated. Tracer kinetic modeling with dynamic ^{18}F-FDG PET imaging has been reported to be useful [7]; however, it is technically difficult to perform as a routine clinical protocol.

In contrast, the standardized uptake value (SUV) is used widely for clinical PET imaging as it is a simpler method for obtaining a semiquantitative index of the amount of ^{18}F-FDG uptake. However, previous research has raised some limitations on standardization of ^{18}F-FDG uptake on PET images as the SUV can be affected by various factors such as body weight, body surface area, lean body mass, and blood glucose level [8]. To improve the accuracy of the SUV in clinical use, a ratio of uptake to a standard reference tissue can potentially improve the diagnostic interpretation by canceling out perturbing factors common to the lesion and the reference site [9]. As mentioned previously, increases in blood glucose levels result in decreased ^{18}F-FDG uptake in normal and tumor tissues through competitive inhibition [10]. Hence, an SUV correction, using the blood glucose level, may be a method to improve the accuracy of the SUV in the detection of residual or recurrent high-grade tumors.

The aim of this study is to assess the accuracies of: SUV corrected by blood glucose level (SUV_{gluc}), the conventional SUV_{max} (normalized by body weight), the SUV ratios to the ipsilateral cerebellar cortex (SUV_{Rc}) and contralateral white matter (SUV_{Rw}), and glucose metabolic rate (GMR) in differentiating the presence of high-grade glioma from post-treatment changes in the monitoring of patients with brain tumors.

Materials and methods

Patients

The review and analysis of the data in this study are retrospective in brain tumor patients who consented to an Institutional Review Board-approved protocol for imaging and data collection. Between February 2010 and December 2012, 230 ^{18}F-FDG PET brain scans were performed for further evaluation of patients with known brain tumors. Eighty-eight cases were excluded because they were nonglioma cases. A total of 42 cases were subsequently disqualified because of the lack of a concurrent MRI within a month's interval of the PET, tumor in the contralateral white matter, tumor in the cerebellum, technically limited study because of patient motion artifact, or uncertainty in the final diagnosis (no subsequent tissue biopsy or insufficient follow-up MRI). We also excluded three cases where the patients were on metformin and also had high blood glucose levels (>170 mg/dl) (Table 1). The remaining 95 lesions were entered in this study and the initial diagnoses on the basis of tissue histology were 88 high-grade gliomas (grade III or IV), seven low-grade gliomas (grade I or II), and two unknown prebiopsy in two lesions (Table 2). The clinical indication for the ^{18}F-FDG PET was for the metabolic evaluation of the patient's brain lesion or lesions, that is detection of residual or recurrent high-grade primary brain tumor. After the PET scan, the patients (lesions) were assigned a final diagnosis (gold standard) on the basis of subsequent histological confirmation (biopsy or resection) or clinical follow-up (frequent MRI) if biopsy results were not available (Table 2). All patients underwent brain MRI with contrast enhancement within 1 month from the date of the ^{18}F-FDG PET scan.

The GMR and the various semiquantitative methods were compared with the 'gold standard'. The lesion was categorized as a postoperative or post-therapy change if on follow-up MRI it decreased in size, showed a decrease in enhancement, or became stable for at least 3 months. Otherwise, the lesion was considered to be residual or a recurrent high-grade tumor. Most of the patients with a diagnosis of a high-grade tumor were under continuous chemotherapy and steroids.

^{18}F-FDG PET imaging

In the 55 patients, 84 PET scans were performed on an ECAT EXACT HR+ (Siemens Medical, Washington DC, USA; 15.5 cm axial field of view, 56.2 cm transaxial field of view, 4.5 mm in-plane and axial resolution, $5 \times 5 \times 5$ mm cross-slice resolution, 2.425 mm interslice distance) and five scans were performed on a Discovery VCT PET/CT (GE Medical Systems, Waukesha, Wisconsin, USA; 15.7 cm axial field of view, 70 cm transaxial field of view, $4.7 \times 6.3 \times 3.27$ mm cross-slice resolution, 3.27 mm interslice distance). Both scanners were American College of Radiology certified to ensure accurate SUV analysis. All patients were instructed to fast for at least 6 h before their scan. Blood glucose levels were measured before the ^{18}F-FDG injection. The patients were

Table 2 Diagnosis of brain lesions

	Initial diagnosis	Final diagnosis
High-grade glioma	88	65
Grade IV (glioblastoma multiforme)	60	49
Grade III glioma	22	15
Grade III/V glioma	6	1
Low-grade (grade I/II) glioma	7	2
Prebiopsy lesion	2	–
Post-treatment change	–	30

positioned in the scanner in a quiet dim room and kept in an unstimulated condition. A 10 min transmission scan obtained with external sources of ^{68}Ge or a low-dose computed tomography (CT) was used for attenuation correction. Patients were injected with ^{18}F-FDG 370 MBq (10 mCi ± 10%) intravenously and a 30-frame dynamic image acquisition for 60 min was simultaneously initiated: 12 frames at 10 s/frame, four frames at 30 s/frame, and 14 frames at 4 min/frame. The image data were reconstructed using the iterative ordered subset expectation maximization (OSEM) method [four iterations, 16 subsets, zoom = 2.5, brain mode on, all pass (ramp) filter, kernel full-width at half-maximum size of 4.0 mm, axial filtering off, and scatter correction on] generating 128 × 128 image matrices (2.06 × 2.06 mm pixel size) for each time frame. For plasma radioactivity measurements, an arterialized venous blood sampling was obtained at 10 min after the ^{18}F-FDG injection using a heated hand box from the University of Vermont. The blood samples were centrifuged and the plasma radioactivity was measured in a gamma well counter to correctly scale the image-derived input function that was obtained from the carotid vessels in the dynamic image data [11].

Parametric images of GMR were generated using the Patlak method applied to the 3–36 min scan interval, a single plasma glucose level, and the assumed lumped constant of 1. Parametric SUV images were generated by summing the last 30 min of the dynamic scan and normalized by the patient's body weight. Parametric SUV_{gluc} images were calculated by multiplying each parametric SUV image pixel by the blood glucose level/100. Both the GMR and the SUV images were coregistered to a recent (< 1 month) brain contrast MRI using mutual information-based software written in IDL (ExelisVisual Information Solutions, Boulder, Colorado, USA).

Image analysis

All images were reviewed visually and further analyzed using the Agfa Impax software (Mortsel, Belgium) by board-certified nuclear medicine physicians and neuroradiologists. The lesion was identified on the MRI and a corresponding region of interest (ROI) was drawn manually on the coregistered transaxial parametric PET images (GMR, SUV_{max}). The maximum pixel value within the ROI of the lesion was recorded for GMR, SUV_{max}, and SUV_{gluc}. The average SUV ROI values were used for the reference structures (ipsilateral cerebellum and contralateral white matter) that were used to calculate the ratios.

Statistical analysis

All data were expressed as mean ± SD. Differences were analyzed using the paired *t*-test (two tailed) and considered to be significant at a *P*-value less than 0.05. To analyze the accuracy of detecting the presence or absence of high-grade tumors, the various quantitative methods were compared with the final true diagnosis on the basis of pathological results or clinical outcome. Appropriate threshold values for each method were selected arbitrarily on the basis of an equal balance in sensitivity and specificity. To avoid the effects of the selected threshold values, the diagnostic accuracies were compared using receiver operating characteristic (ROC) analysis with ROCKIT (1.1B2; University of Chicago, Chicago, Illinois, USA).

Results

Histopathological analysis and patient follow-up

From the total of 97 lesions, 33 were subjected to biopsy or either partial, subtotal, or gross total resection within 6 months after ^{18}F-FDG PET, which allowed the final diagnoses to be confirmed pathologically. The other 64 lesions were diagnosed clinically through follow-up with contrast-enhanced MRI images taken at intervals of several months.

In 18 lesions, the GMR was not available because of the absence of a dynamic brain acquisition, difficulties in blood draw, or lack of calibration between the well counter and the scanner. The SUV_{max} and SUV_{gluc} were not available in one patient because of a lack of calibration between the dose calibrator and the scanner. The detailed final true diagnosis is presented in Table 2. Post-treatment changes included radiation injury and postsurgical changes.

Diagnostic value of GMR, SUV, SUV_{gluc}, SUV_{Rc}, and SUV_{Rw}

Results from the final true diagnosis were compared with the quantitative and semiquantitative results from ^{18}F-FDG PET imaging (Table 3). There was clear separation of the mean values of SUV_{max}, SUV_{Rc}, SUV_{Rw}, SUV_{gluc}, and GMR between the presence of high-grade glioma and postoperative change or low-grade glioma (Fig. 1). All methods were statistically significant ($P < 0.01$).

The results of the ROC analysis (Fig. 2) showed that the SUV_{gluc} was a more reliable method than the conventional SUV_{max} method for distinguishing high-grade gliomas from post-treatment changes and low-grade

Table 3 Characteristics of brain lesions

	High-grade tumor ($n = 65$)	Post-treatment change or low-grade glioma ($n = 32$)
Patient age (years)	27–77 (average 53.7)	25–73 (average 58.9)
Plasma glucose (mg/dl)	105.4 ± 27.2	95.6 ± 19.6
SUV_{max}	6.12 ± 2.33	3.68 ± 1.47
SUV_{Rc}	1.26 ± 0.48	0.71 ± 0.30
SUV_{Rw}	2.47 ± 0.95	1.39 ± 0.44
SUV_{gluc}	6.23 ± 2.39	3.40 ± 1.27
GMR (μmol/min/100 g)	18.11 ± 10.37	9.45 ± 3.38

GMR, glucose metabolic rate; SUV_{gluc}, glucose-corrected standardized uptake value; SUV_{max}, maximum value of the standardized uptake value; SUV_{Rc}, standardized uptake value ratios to the ipsilateral cerebellar cortex; SUV_{Rw}, standardized uptake value ratios to the contralateral white matter.

Fig. 1

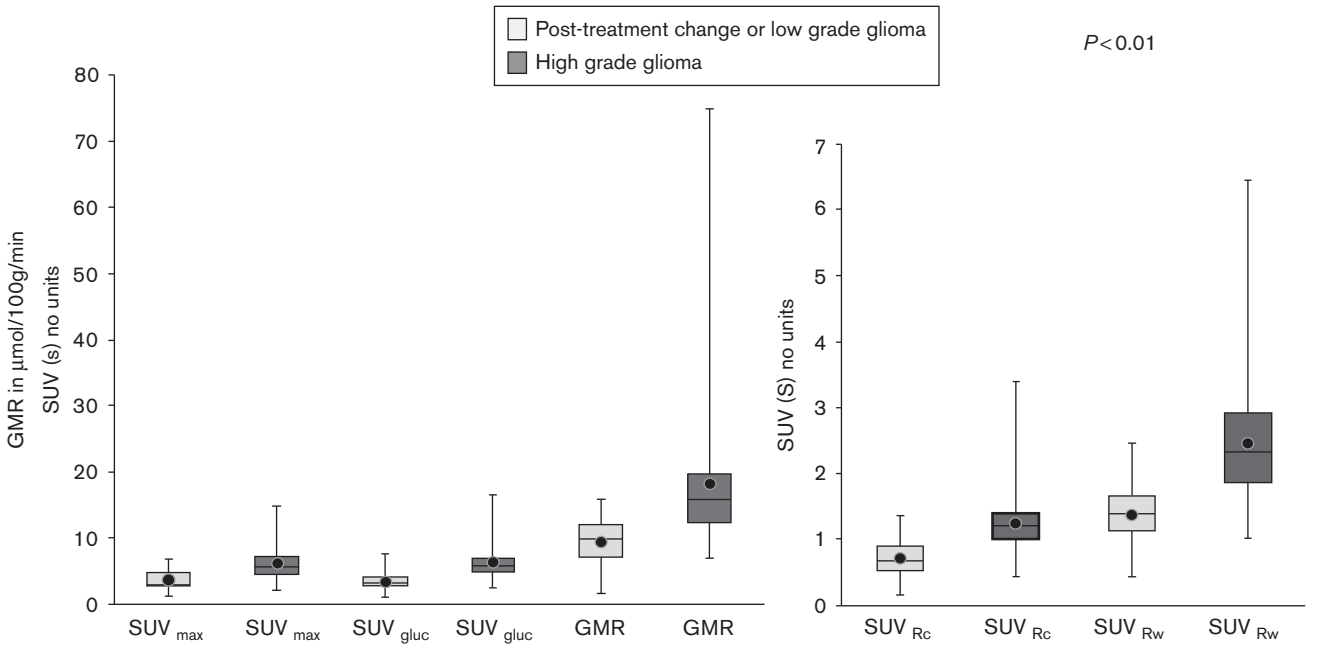

Box and whisker plots of SUV_{max}, SUV_{Rc}, SUV_{Rw}, SUV_{gluc}, and GMR for post-treatment change and low-grade glioma and for high-grade glioma. The difference in the mean values between two categories was significant for all the methods tested. ^{18}F-FDG, fluorine-18 fluorodeoxyglucose; GMR, glucose metabolic rate; ROC, receiver operating characteristic curve; SUV_{gluc}, glucose-corrected standardized uptake value; SUV_{max}, maximum value of the standardized uptake value; SUV_{Rc}, standardized uptake value ratios to the ipsilateral cerebellar cortex; SUV_{Rw}, standardized uptake value ratios to the contralateral white matter.

Fig. 2

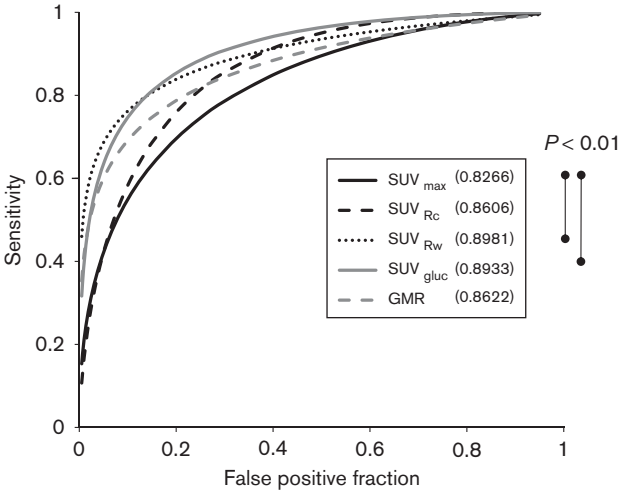

The ROC curves of SUV_{max}, SUV_{Rc}, SUV_{Rw}, SUV_{gluc}, and GMR. SUV_{Rw}, and SUV_{gluc} have better areas under the curve (0.8981 and 0.8933, respectively) than the conventional SUV_{max} method ($P < 0.01$) for distinguishing high-grade glioma from post-treatment change and low-grade glioma. The comparison between the other methods was not statistically significant. For abbreviations, see Fig. 1 legend.

gliomas ($P = 0.0029$). However, the SUV_{gluc} was not significantly different from the SUV_{Rc}, SUV_{Rw}, or GMR. Using a threshold of 4.3 for the SUV_{gluc}, the sensitivity was 80% (52/65), specificity was 81% (25/31), and accuracy was 80% (77/96) (Table 4).

There were 13 false-negative lesions for the SUV_{gluc} where the high-grade gliomas had SUV_{gluc} of equal to or less than 4.3, but were positive on the basis of pathology ($n = 4$) and clinical outcome ($n = 9$). The pathological or clinical diagnoses were glioblastoma multiforme (GBM) ($n = 10$) and anaplastic astrocytoma ($n = 3$). In 10 of the 13 lesions, the conventional SUV_{max} was also false negative. The blood glucose in this group was between 71 and 190 mg/dl.

There were six patients with false-positive lesions using the SUV_{gluc} where the SUV_{gluc} was greater than the 4.3 threshold but the lesions were negative for high-grade glioma on the basis of pathological confirmation ($n = 1$) and clinical follow-up ($n = 5$). Four out of six patients had a history of surgery or radiation therapy within 2 months before the PET scan. Five out of six patients also had a false-positive conventional SUV_{max}. The blood glucose level in this group was between 82 and 121 mg/dl.

On the ROC curve analysis (Fig. 2), the area under curve for SUV_{gluc}, SUV_{Rc}, SUV_{Rw}, and GMR were 0.8933, 0.8606, 0.8981, and 0.8622, respectively. The conventional SUV_{max} had the lowest area under the ROC curve of 0.8266. The sensitivity, specificity, and accuracy are shown in Table 4.

Table 4 Receiver operating curve analysis for predicting viable high-grade gliomas

	SUV_{max}	SUV_{Rc}	SUV_{Rw}	SUV_{gluc}	GMR
Cut-off value	> 4.6	> 0.9	> 1.8	> 4.3	> 12.2
Sensitivity (%)	72 (47/65)	77 (50/65)	79 (51/65)	80 (52/65)	78 (42/54)
Specificity (%)	71 (22/31)	75 (24/32)	84 (27/32)	81 (25/31)	76 (19/25)
Accuracy (%)	72 (69/96)	76 (74/97)	80 (78/97)	80 (77/96)	77 (61/79)
Area under curve	0.8266	0.8606	0.8981	0.8933	0.8622

GMR, glucose metabolic rate; SUV_{gluc}, glucose-corrected standardized uptake value; SUV_{max}, maximum value of the standardized uptake value; SUV_{Rc}, standardized uptake value ratios to the ipsilateral cerebellar cortex; SUV_{Rw}, standardized uptake value ratios to the contralateral white matter.

The parametric images of GMR visually showed more noise compared with the SUV images. This is expected as the GMR values are derived from the Patlak graphical method. SUV and SUV_{gluc} parametric images were relatively less noisy as they are simply rescaled summed images and only differ in their intensity scaling factor. A patient with high-grade glioma correctly identified by a parametric SUV_{gluc} and GMR image, but incorrectly identified as post-treatment change by SUV_{max} is shown in Fig. 3. A patient with post-treatment changes correctly identified by a parametric SUV_{gluc} and GMR image, but incorrectly identified as high-grade tumor by SUV_{max} is shown in Fig. 4.

Discussion

Differentiation of high-grade tumors from post-treatment changes can be challenging because of the similar appearance of contrast enhancement on MRI. Postsurgical changes, postradiation changes, and pseudoprogression after chemotherapy can appear similar to residual or recurrent high-grade gliomas. Therefore, standard MRI cannot accurately distinguish between these two entities [12]. There are advanced MRI techniques, such as proton MR spectroscopy (^{1}H-MRS) and perfusion MRI, which show promise in distinguishing recurrent glioma from treatment effect [13–15]. However, ^{1}H-MRS has limited value in detecting small tumors and in evaluating lesions adjacent to scalp, ventricles, calcified structures, surgical clips, and hemorrhage. Limitations of perfusion MRI include the possible underestimation of tumor perfusion because of contrast leakage through an impaired blood–brain barrier [16]. ^{18}F-FDG PET and more recently ^{18}F-FDG PET/CT have been used to help distinguish these lesions.

The fundamental principle that there is increased metabolism in malignant cells compared with normal or benign tissues can also be applied in gliomas. Another theoretical advantage for PET is that alterations in tumor cell metabolism may show earlier changes compared with anatomic changes in size when a tumor responds to therapy. In addition, some therapeutic agents are cytostatic rather than cytoreductive, making post-treatment evaluation challenging when only morphologic imaging modalities are used.

Formal quantitative ^{18}F-FDG imaging such as the GMR method in this study has previously been reported to be useful [7]. One proposed explanation is that malignant cells have a higher concentration of hexokinase, resulting in a higher rate of glycolysis compared with normal tissues and benign lesions [17]. Goldman *et al.* [18] reported that the GMR correlates with the histopathological malignancy grade in brain tumors. In accordance with their observation, we obtained similar results. However, the technical requirements for a quantitative study are complex and time consuming and not feasible for routine clinical imaging. As an alternative to the calculation of the GMR, the SUV_{max} is used widely as a simple metric of ^{18}F-FDG uptake. However, our results of ROC analysis showed that the area under curve of the SUV_{max} was lower than the other methods that we applied to the brain lesions. To overcome the limitations of the SUV_{max}, many alternative semiquantitative methods have been reported in the evaluation of brain gliomas with ^{18}F-FDG PET [4,18–22].

A variety of biologic and technical factors can affect the SUV measurements. Some factors, such as blood glucose level and muscular activity, can be controlled at the time of tracer administration. However, most are impossible to define in any individual case. Comparison of uptake with a standard reference tissue, if available, can potentially improve the diagnostic performance of a method by canceling out perturbing factors common to the lesion and the reference tissue [9]. In our study, we chose the ipsilateral cerebellar cortex and contralateral white matter as reference tissues because they have a relatively stable metabolism. Our results showed that the SUV_{Rc} method had a ROC area under the curve similar to that of the GMR method.

We corrected the SUV with the patients' blood glucose level as another method for compensation for variations and effect of blood glucose on ^{18}F-FDG uptake, similar to the underlying calculation of the GMR from the Patlak method. Our results show that the SUV_{max} has the lowest diagnostic accuracy among the various methods and the SUV_{gluc} and the SUV_{Rw} show the highest accuracies. These results are similar to those of the previous studies differentiating malignant brain lesions from benign lesions [23]. Although there are several previous

Fig. 3

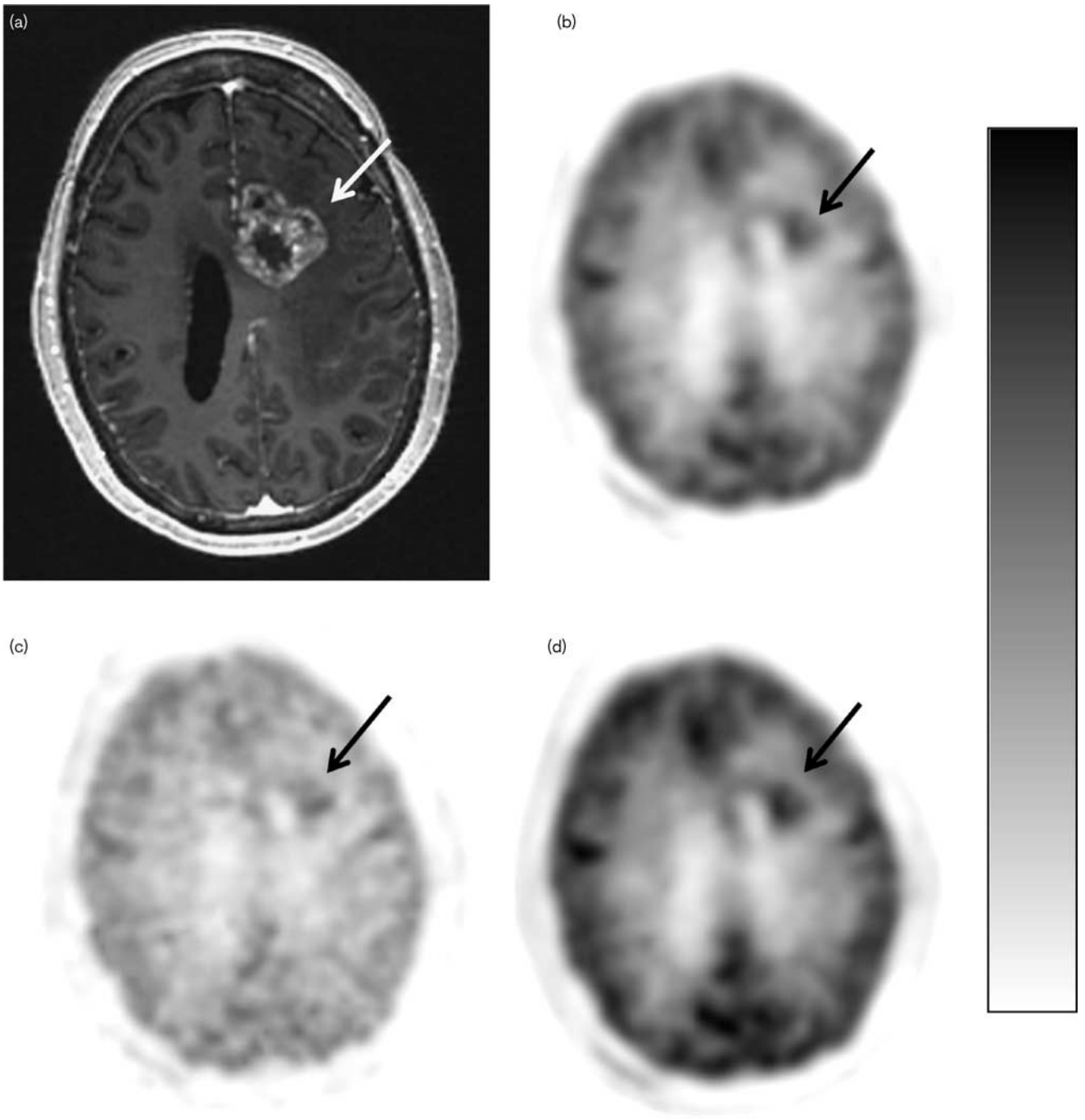

Scanning images of a 55-year-old woman with possible recurrent glioblastoma, status postgross total resection, and chemoradiation. (a) Postcontrast axial T1-weighted MR image shows enhancement in the left frontal lobe (arrow). (b) SUV_{max} axial ^{18}F-FDG PET image with lesion uptake = 3.91 (arrow). (c) GMR parametric axial ^{18}F-FDG PET image shows focal uptake [15.35 μmol glucose/min/100 g (arrow)]. (d) Axial SUV_{gluc} ^{18}F-FDG PET image, measured uptake value = 5.74 (arrow). For abbreviations, see Fig. 1 legend.

publications discussing the effects of abnormal blood glucose levels on tumor and normal brain uptake [24], no previous publication has reported the application of the SUV_{gluc} to differentiate residual or recurrent high-grade glioma from post-treatment change. This study shows that SUV_{gluc} may be a reliable and simple method because the patient's blood glucose level is usually available as it is measured as part of routine clinical protocols. Correction of the SUV by the blood glucose level is also mentioned in the EANM procedure

Fig. 4

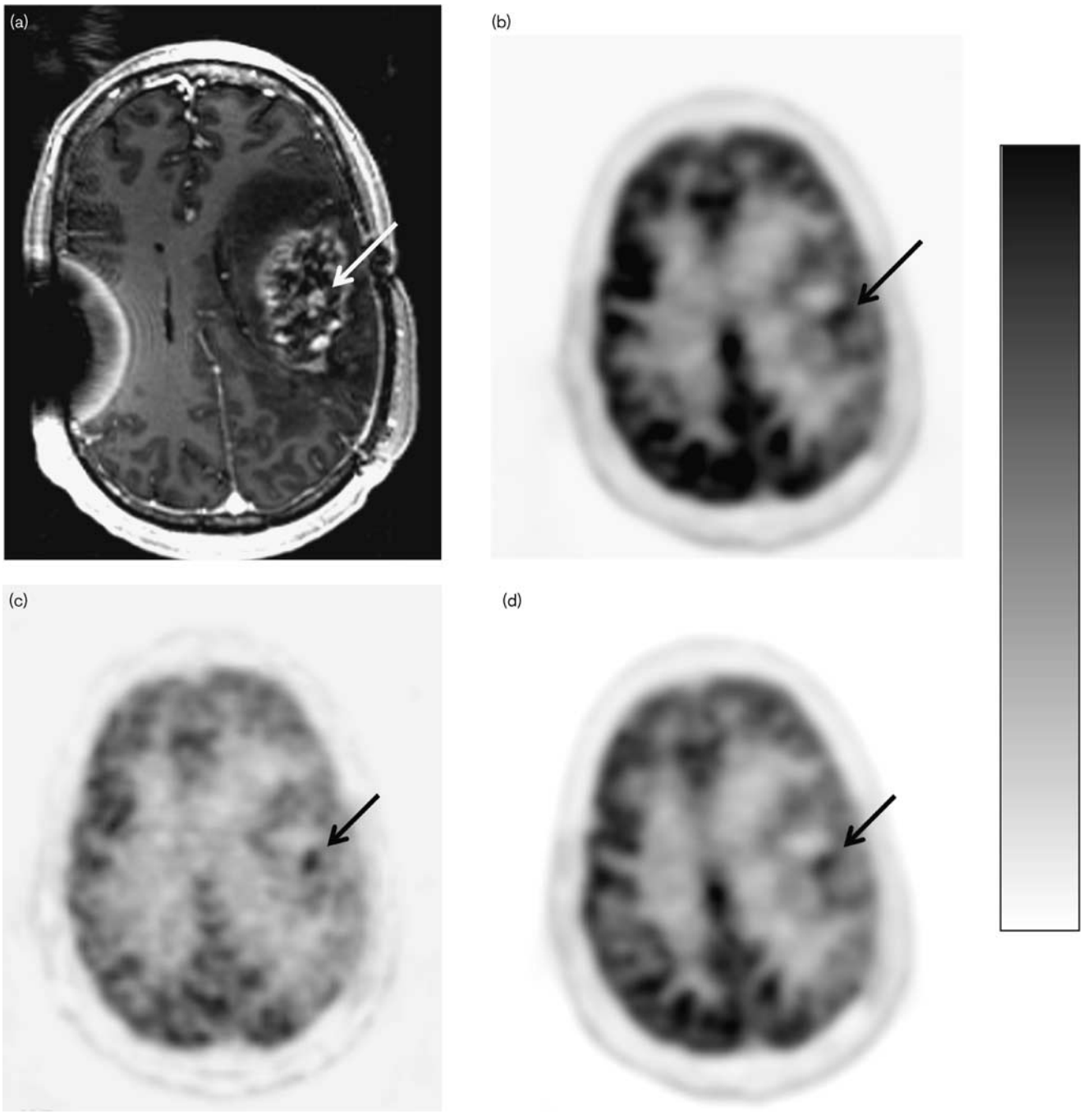

Scanning images of a 43-year-old man with high-grade glioma, status postgross total resection and chemoradiation. (a) Postcontrast axial T1-weighted MR image shows enhancement in the left frontoparietal area (arrow). (b) SUV_{max} axial ^{18}F-FDG PET parametric image, lesion uptake = 6.54 (arrow). (c) GMR parametric axial ^{18}F-FDG PET image shows focal uptake [10.21 μmol glucose/min/100 g (arrow)]. (d) Axial SUV_{gluc} ^{18}F-FDG PET image, measured uptake value = 4.25 (arrow). For abbreviations, see Fig. 1 legend.

guidelines for PET brain imaging [25]; however, no specific correction methods or threshold SUV_{gluc} values are presented. Moreover, the SUV_{gluc} requires no additional reference ROI to be defined in its calculation and can be generated automatically as a parametric image.

Patients with gliomas are frequently treated with steroids to reduce brain edema; however, steroids can cause diabetes mellitus and increase blood glucose level, which can then affect the ^{18}F-FDG uptake in the brain. In our study, four patients with false-negative SUV_{max} had high

blood glucose level (>140 mg/dl), but were diagnosed successfully by the SUV_{gluc}. However, antidiabetic drugs may cause hypoglycemia. There were three lesions with false-positive SUV_{max} in patients with hypoglycemia (<70 mg/dl); however, these lesions were diagnosed correctly by the SUV_{gluc}.

Our study has several limitations. First, the patients' true histological diagnosis at the time of each imaging study was rarely available. The time between ^{18}F-FDG PET scan and biopsy or resection varied from several days to 6 months depending on the patients' status and other imaging findings. Even if the patients undergo a biopsy or resection shortly after the PET scan, the exact anatomic location of the specimen may not correspond to the location of abnormal imaging findings. Second, without tissue biopsy, use of the clinical follow-up and MRI follow-up has its own limitations. We considered the lesion to represent post-treatment changes or residual low-grade glioma if it became smaller, had an interval decrease in enhancement, or was stable on MRI for at least 3 months. However, this MRI appearance may also be found in patients with tumor progression (pseudoresponse) following angiogenic therapy such as bevacizumab [26]. In contrast, the typical MRI findings for tumor progression, such as interval increased enhancement and edema, can be seen in pseudoprogression, when there is actually no tumor progression. Pseudoprogression may be a result of multiple confounding factors that include radiation injury, temozolomide-based chemoradiation, and local glioma therapy. Repeat MRIs can be useful to diagnose pseudoprogression and pseudoresponse as very rapid changes are not typically seen in real tumor progression [27]. Third, 13 patients in our study were administered metformin, which may affect ^{18}F-FDG uptake such that it cannot be corrected by adjusting for their blood glucose level. Metformin is an oral antidiabetic drug in the biguanide class and used widely for the treatment of type 2 diabetes. It is also known for its antitumor effect on glioma [28] and could be used with temozolomide-based chemotherapy as an adjuvant treatment for high-grade gliomas [29]. Tissue glucose utilization is believed to be enhanced by metformin. In-vivo and in-vitro studies have shown that metformin stimulates the insulin-induced glucose uptake into skeletal muscle and adipocytes in both diabetic individuals and animal models. It has also been shown that insulin-mediated visceral fat glucose uptake is enhanced by metformin monotherapy, which is believed to be related to enhancement in visceral fat insulin sensitivity. There have been recommendations to discontinue metformin at least 12 h before carrying out a PET study [30]. We excluded three lesions in patients who were on metformin and had a high blood glucose level (>170 mg/dl) because metformin produces a dose-dependent increase in tumor glucose uptake [31] and the high blood glucose level causes the SUV_{gluc} to be overcorrected.

Despite several limitations, the results in our study confirmed that SUV_{gluc} is more reliable than the conventional SUV. This method saves the complexity of calculating the GMR or defining an additional reference region. The SUV_{gluc} method may aid in the differentiation between residual or recurrent high-grade glioma and post-treatment changes.

Acknowledgements

This research was supported in part by the Wagner Torizuka Fellowship Program and Gifu Prefectural General Medical Center to A. Nozawa and by grants from National Institutes of Health (NIH3P30CA023100-25S8) and from UC San Diego Brain Cancer Research Funds to S. Kesari.

Conflicts of interest

There are no conflicts of interest.

References

1 Tezcan Y, Koc M. 3-D conformal radiotherapy with concomitant and adjuvant temozolomide for patients with glioblastoma multiforme and evaluation of prognostic factors. *Radiol Oncol* 2011; **45**:213–219.
2 Kim YH, Oh SW, Lim YJ, Park CK, Lee SH, Kang KW, *et al*. Differentiating radiation necrosis from tumor recurrence in high-grade gliomas: assessing the efficacy of ^{18}F-FDG PET, ^{11}C-methionine PET and perfusion MRI. *Clin Neurol Neurosurg* 2010; **112**:758–765.
3 Stupp R, Mason WP, van den Bent MJ, Weller M, Fisher B, Taphoorn MJ, *et al*. European Organisation for Research and Treatment of Cancer Brain Tumor and Radiotherapy Groups; National Cancer Institute of Canada Clinical Trials Group. Radiotherapy plus concomitant and adjuvant temozolomide for glioblastoma. *N Engl J Med* 2005; **352**:987–996.
4 Kosaka N, Tsuchida T, Uematsu H, Kimura H, Okazawa H, Itoh H. ^{18}F-FDG PET of common enhancing malignant brain tumors. *Am J Roentgenol* 2008; **190**:W365–W369.
5 Wu HM, Bergsneider M, Glenn TC, Yeh E, Hovda DA, Phelps ME, *et al*. Measurement of the global lumped constant for 2-deoxy-2-[^{18}F]fluoro-D-glucose in normal human brain using [^{15}O]water and 2-deoxy-2-[^{18}F]fluoro-D-glucose positron emission tomography imaging. A method with validation based on multiple methodologies. *Mol Imaging Biol* 2003; **5**:32–41.
6 Phelps ME, Huang SC, Hoffman EJ, Selin C, Sokoloff L, Kuhl DE. Tomographic measurement of local cerebral glucose metabolic rate in humans with (F-18)2-fluoro-2-deoxy-D-glucose: validation of method. *Ann Neurol* 1979; **6**:371–388.
7 Kimura N, Yamamoto Y, Kameyama R, Hatakeyama T, Kawai N, Nishiyama Y. Diagnostic value of kinetic analysis using dynamic ^{18}F-FDG-PET in patients with malignant primary brain tumor. *Nucl Med Commun* 2009; **30**:602–609.
8 Boellaard R. Standards for PET image acquisition and quantitative data analysis. *J Nucl Med* 2009; **50**:11S–20S.
9 Britz-Cunningham SH, Millstine JW, Gerbaudo VH, Britz-Cunningham SH, Millstine JW, Gerbaudo VH, *et al*. Improved discrimination of benign and malignant lesions on FDG PET/CT, using comparative activity ratios to brain, basal ganglia, or cerebellum. *Clin Nucl Med* 2008; **33**:681–687.
10 Lee SM, Kim TS, Lee JW, Kim SK, Park SJ, Han SS. Improved prognostic value of standardized uptake value corrected for blood glucose level in pancreatic cancer using F-18 FDG PET. *Clin Nucl Med* 2011; **36**: 331–336.
11 Schiepers C, Hoh C, Dahlbom M, Wu H, Phelps M. Factor analysis for delineation of organ structures, creation of input and output functions, and standardization of multi-center kinetic modeling. *Proc SPIE* 1999; **3661**:1343–1350.
12 Yang I, Huh NG, Smith ZA, Han SJ, Parsa AT. Distinguishing glioma recurrence from treatment effect after radiochemotherapy and immunotherapy. *Neurosurg Clin N Am* 2010; **21**:181–186.

13 Hu LS, Baxter LC, Smith KA, Feuerstein BG, Karis JP, Eschbacher JM*, et al*. Relative cerebral blood volume values to differentiate high-grade glioma recurrence from posttreatment radiation effect: direct correlation between image-guided tissue histopathology and localized dynamic susceptibility-weighted contrast-enhanced perfusion MR imaging measurements. *Am J Neuroradiol* 2009; **30**:552–558.
14 Barajas RF Jr, Chang JS, Segal MR, Parsa AT, McDermott MW, Berger MS, Cha S. Differentiation of recurrent glioblastoma multiforme from radiation necrosis after external beam radiation therapy with dynamic susceptibility-weighted contrast-enhanced perfusion MR imaging. *Radiology* 2009; **253**:486–496.
15 Bobek-Billewicz B, Stasik-Pres G, Majchrzak H, Zarudzki L. Differentiation between brain tumor recurrence and radiation injury using perfusion, diffusion-weighted imaging and MR spectroscopy. *Folia Neuropathol* 2010; **48**:81–92.
16 Dhermain FG, Hau P, Lanfermann H, Jacobs AH, van den Bent MJ. Advanced MRI and PET imaging for assessment of treatment response in patients with gliomas. *Lancet Neurol* 2010; **9**:906–920.
17 Wu H, Dimitrakopoulou-Strauss A, Heichel TO, Lehner B, Bernd L, Ewerbeck V*, et al*. Quantitative evaluation of skeletal tumours with dynamic FDG PET: SUV in comparison to Patlak analysis. *Eur J Nucl Med* 2001; **28**:704–710.
18 Goldman S, Levivier M, Pirotte B, Brucher JM, Wikler D, Damhaut P*, et al*. Regional glucose metabolism and histopathology of gliomas. A study based on positron emission tomography-guided stereotactic biopsy. *Cancer* 1996; **78**:1098–1106.
19 Hustinx R, Smith RJ, Benard F, Bhatnagar A, Alavi A. Can the standardized uptake value characterize primary brain tumors on FDG-PET? *Eur J Nucl Med* 1999; **26**:1501–1509.
20 Delbeke D, Meyerowitz C, Lapidus RL, Maciunas RJ, Jennings MT, Moots PL, Kessler RM. Optimal cutoff levels of F-18 fluorodeoxyglucose uptake in the differentiation of low-grade from high-grade brain tumors with PET. *Radiology* 1995; **195**:47–52.
21 Barker FG 2nd, Chang SM, Valk PE, Pounds TR, Prados MD. 18-Fluorodeoxyglucose uptake and survival of patients with suspected recurrent malignant glioma. *Cancer* 1997; **79**:115–126.
22 Prieto E, Marti-Climent JM, Dominguez-Prado I, Garrastachu P, Díez-Valle R, Tejada S*, et al*. Voxel-based analysis of dual-time-point ^{18}F-FDG PET images for brain tumor identification and delineation. *J Nucl Med* 2011; **52**: 865–872.
23 Nozawa A, Rivandi AH, Kesari S, Hoh CK. Glucose corrected standardized uptake value (SUV_{gluc}) in the evaluation of brain lesions with ^{18}F-FDG PET. *Eur J Nucl Med Mol Imaging* 2013; **40**:997–1004.
24 Ishizu K, Nishizawa S, Yonekura Y, Sadato N, Magata Y, Tamaki N*, et al*. Effects of hyperglycemia on FDG uptake in human brain and glioma. *J Nucl Med* 1994; **35**:1104–1109.
25 Varrone A, Asenbaum S, Borght T, Booij J, Nobili F, Någren K*, et al*. EANM procedure guidelines for PET brain imaging using [^{18}F]FDG, version 2. *Eur J Nucl Med Mol Imaging* 2009; **36**:2103–2110.
26 Fink J, Born D, Chamberlain MC. Pseudoprogression: relevance with respect to treatment of high-grade gliomas. *Curr Treat Options Oncol* 2011; **12**:240–252.
27 Brandsma D, van den Bent MJ. Pseudoprogression and pseudoresponse in the treatment of gliomas. *Curr Opin Neurol* 2009; **22**:633–638.
28 Gao LB, Tian S, Gao HH, Xu YY. Metformin inhibits glioma cell U251 invasion by downregulation of fibulin-3. *Neuroreport* 2013; **24**:504–508.
29 Soritau O, Tomuleasa C, Aldea M, Petrushev B, Susman S, Gheban D*, et al*. Metformin plus temozolomide-based chemotherapy as adjuvant treatment for WHO grade III and IV malignant gliomas. *J BUON* 2011; **16**:282–289.
30 Bahar Dasgeb ES. Alteration of FDG uptake associated with metformin Pitfall and opportunity. *J Nucl Med* 2007; **48** (Suppl 2):184P.
31 Habibollahi P, van den Berg NS, Kuruppu D, Loda M, Mahmood U. Metformin – an adjunct antineoplastic therapy – divergently modulates tumor metabolism and proliferation, interfering with early response prediction by ^{18}F-FDG PET imaging. *J Nucl Med* 2013; **54**:252–258.